Article

Cell Reports

Deposition of 5-Methylcytosine on Enhancer RNAs Enables the Coactivator Function of PGC-1α

Graphical Abstract

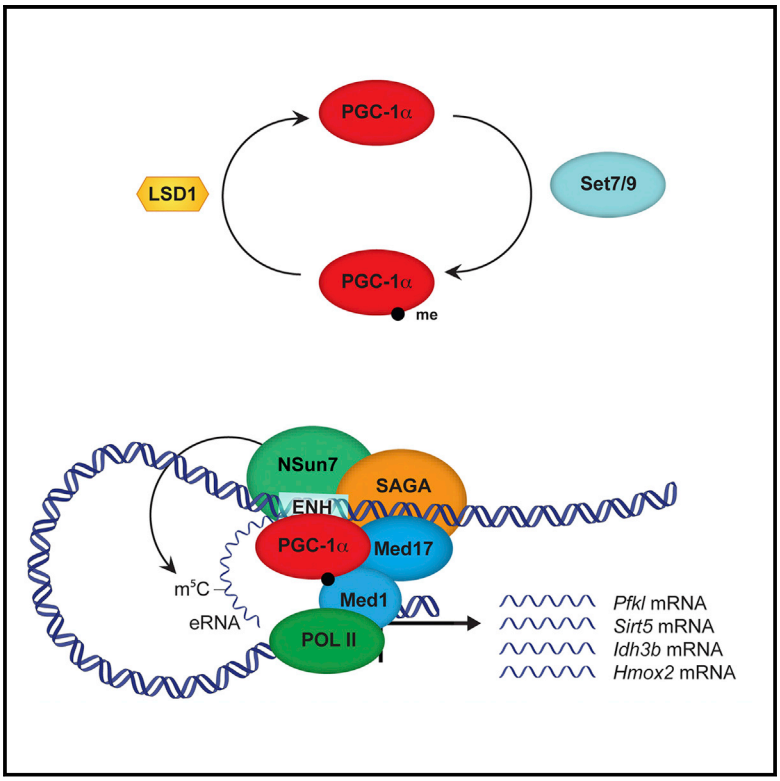

Authors

Francesca Aguilo, SiDe Li, Natarajan Balasubramaniyan, ..., Weijia Zhang, Frederick J. Suchy, Martin J. Walsh

Correspondence

martin.walsh@mssm.edu

In Brief

Aguilo et al. find that PGC-1α can regulate metabolic networks that integrate the modification of PGC-1α, NSUN7 and m^5C-modified eRNAs. These findings illustrate how complex epigenetic circuitry might function to fine-tune metabolic responses through the PGC-1α co-activator.

Highlights

- K779 of PGC-1α is methylated by SET7/9 and demethylated by LSD1
- PGC-1α[K779me] recruits SAGA and Mediator at enhancers of target genes
- PGC-1α[K779me] corresponds with NSUN7 and m^5C eRNAs at PGC1α-regulated loci
- Enrichment of m^5C within eRNA coincides with fasting in vivo

Accession Numbers

GSE57852

Aguilo et al., 2016, Cell Reports *14*, 479–492
January 26, 2016 ©2016 The Authors
http://dx.doi.org/10.1016/j.celrep.2015.12.043

Cell Reports
Article

OPEN ACCESS
CellPress

Deposition of 5-Methylcytosine on Enhancer RNAs Enables the Coactivator Function of PGC-1α

Francesca Aguilo,[1,2,8] SiDe Li,[1,8] Natarajan Balasubramaniyan,[5,8] Ana Sancho,[1,2] Sabina Benko,[1,2] Fan Zhang,[4] Ajay Vashisht,[6] Madhumitha Rengasamy,[1,2] Blanca Andino,[1,2] Chih-hung Chen,[1,2] Felix Zhou,[2] Chengmin Qian,[7] Ming-Ming Zhou,[2] James A. Wohlschlegel,[6] Weijia Zhang,[4] Frederick J. Suchy,[5] and Martin J. Walsh[1,2,3,*]
[1]Department of Pediatrics
[2]Department of Structural and Chemical Biology
[3]Department of Genetics and Genomic Sciences
[4]Division of Nephrology, Department of Medicine, Laboratory of Bioinformatics
Icahn School of Medicine at Mount Sinai, New York, NY 10029, USA
[5]Children's Hospital Research Institute of Colorado, University of Colorado School of Medicine, Aurora, CO 80045, USA
[6]Department of Biological Chemistry and Institute of Genomics and Proteomics, University of California, Los Angeles, Los Angeles, CA 90095, USA
[7]Department of Biochemistry, Lin Ka Shing Faculty of Medicine, University of Hong Kong, Hong Kong, PRC
[8]Co-first author
*Correspondence: martin.walsh@mssm.edu
http://dx.doi.org/10.1016/j.celrep.2015.12.043
This is an open access article under the CC BY-NC-ND license (http://creativecommons.org/licenses/by-nc-nd/4.0/).

SUMMARY

The Peroxisome proliferator-activated receptor-gamma coactivator 1 alpha (PGC-1α) is a transcriptional co-activator that plays a central role in adapted metabolic responses. PGC-1α is dynamically methylated and unmethylated at the residue K779 by the methyltransferase SET7/9 and the Lysine Specific Demethylase 1A (LSD1), respectively. Interactions of methylated PGC-1α[K779me] with the Spt-Ada-Gcn5-acetyltransferase (SAGA) complex, the Mediator members MED1 and MED17, and the NOP2/Sun RNA methytransferase 7 (NSUN7) reinforce transcription, and are concomitant with the m^5C mark on enhancer RNAs (eRNAs). Consistently, loss of *Set7/9* and *NSun7* in liver cell model systems resulted in depletion of the PGC-1α target genes *Pfkl*, *Sirt5*, *Idh3b*, and *Hmox2,* which was accompanied by a decrease in the eRNAs levels associated with these loci. Enrichment of m^5C within eRNA species coincides with metabolic stress of fasting in vivo. Collectively, these findings illustrate the complex epigenetic circuitry imposed by PGC-1α at the eRNA level to fine-tune energy metabolism.

INTRODUCTION

Processes that contribute to a rapid transcriptional response when the biological need for energy arises converge on the Peroxisome proliferator-activated receptor-gamma coactivator 1 alpha (PGC-1α) (Finck and Kelly, 2006; Knutti and Kralli, 2001; Lin et al., 2005; Lowell and Spiegelman, 2000; Rosenfeld et al., 2006; Scarpulla, 2008). PGC-1α is a transcriptional co-activator that interacts with selective transcription factors and chromatin-remodeling complexes to modulate the transcription of target genes (Aubert et al., 2009). Because PGC-1α has a highly conserved and functional RNA recognition motif (RRM) (Monsalve et al., 2000), interactions with enhancer-associated RNAs (eRNAs), tethering critical proteins to chromatin, could regulate an adaptive metabolic response in an alternative manner (Natoli and Andrau, 2012; Shiekhattar, 2013).

Biological models illustrating the role of epigenetic and post-translational modifications of co-activators and co-repressor as functional signatures for transcriptional activity have emerged (Berger, 2002, 2007; Jenuwein and Allis, 2001; Rosenfeld et al., 2006). PGC-1α is acetylated by the histone acetyltransferase GCN5 of the Spt-Ada-Gcn5-acetyltransferase (SAGA) complex (Kelly et al., 2009; Lerin et al., 2006), deacetylated by SIRT1 (Nemoto et al., 2005; Rodgers et al., 2005), serine phosphorylated by AKT/PKB (Li et al., 2007), AMPK, p38 MAPK, and GSK3β (Fernandez-Marcos and Auwerx, 2011), and asymmetrically dimethylated by PRMT1 (Teyssier et al., 2005). These post-translational modifications can occur in an exclusive or combined manner, and may reinforce or diminish the potential of PGC-1α to co-activate transcription under diverse metabolic conditions (Cantó and Auwerx, 2009), resulting in defective control of multiple transcriptional networks (Lerin et al., 2006; Li et al., 2007; Teyssier et al., 2005). On the other hand, lysine methylation by the histone mono-methyltransferase SET7/9, and lysine demethylation by the Lysine Specific Demethylase 1 (LSD1), have been shown to play an important role in non-histone proteins such as p53 and DNMT1 (Chuikov et al., 2004; Estève et al., 2009; Nicholson and Chen, 2009; Pradhan et al., 2009; Wang et al., 2009).

Chemical modification also occurs on RNA, functioning as a sensor of the metabolic status to influence gene regulatory networks at the epigenetic level (Towns and Begley, 2012). The NOL1/NOP2/Sun (*NSun*) domain-containing genes encode the

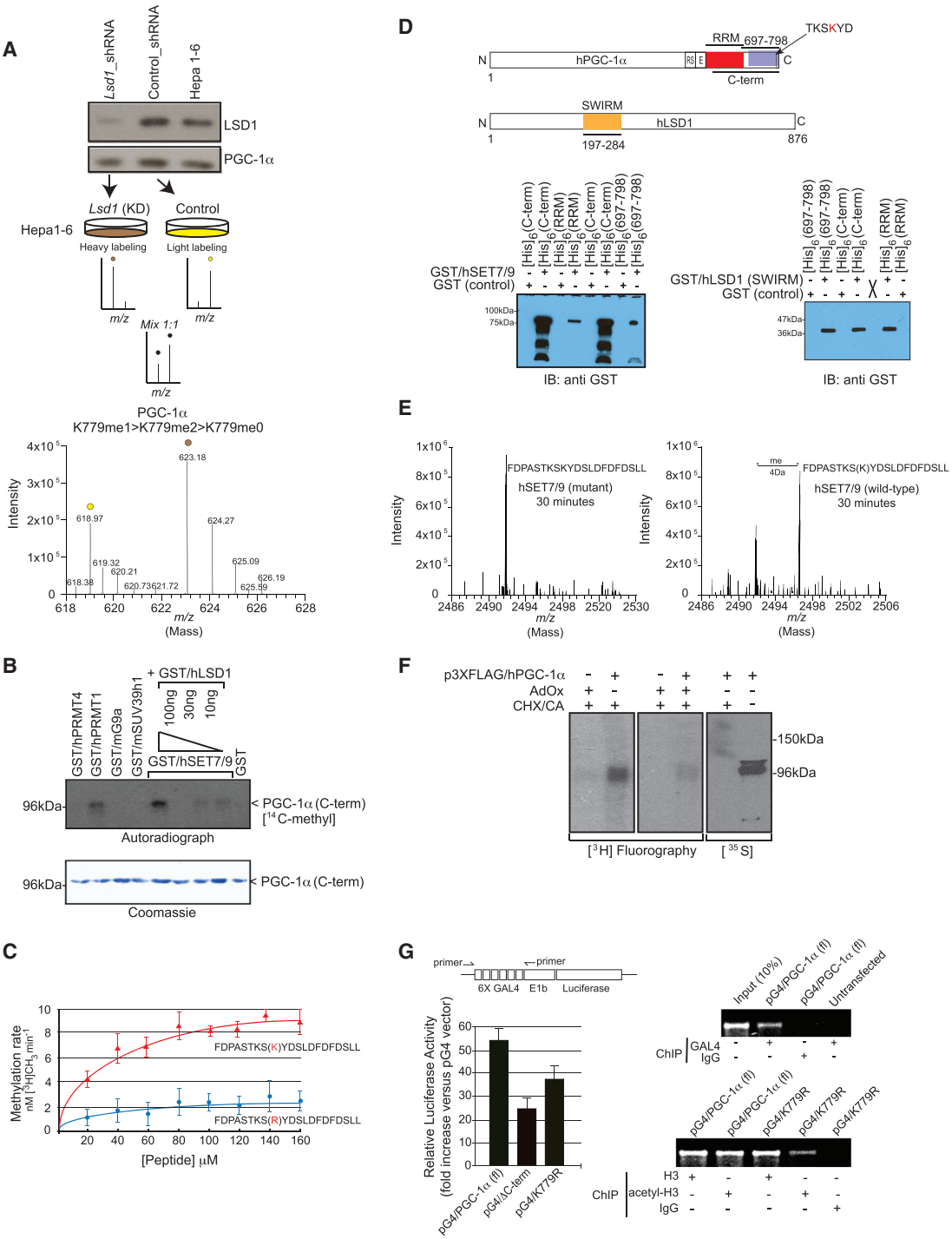

Figure 1. PGC-1α Is a Direct Substrate for LSD1 and SET7/9 and the Methylation State Is Associated with Enhanced Transcription Activation

(A) LSD1 and PGC-1α western blot of nuclear extracts from Hepa 1-6 infected with control or *Lsd1* shRNA (upper). These nuclear extracts were used for SILAC assays (below). The mass spectra revealed PGC-1α as a significant substrate for LSD1.

(B) Autoradiography for in vitro methylation assays performed with the recombinant C-terminal domain of the human PGC-1α protein and the recombinant methyltransferases indicated in the figure. For the demethylation assay, recombinant C-terminal domain of the human PGC-1α was incubated with a constant amount of SET7/9 and increased amounts of LSD1. Coomassie staining was used as a loading control (lower).

(C) Steady-state kinetic analysis of wild-type PGC-1α[K779] and mutant PGC-1α[K779R] peptides for in vitro reactions with recombinant SET7/9 enzyme.

(D) Direct interaction studies of $[His]_6$-tagged C-terminal domain (C-term), RNA recognition motif (RRM), or amino acids 697 to 798 (697–798) of human PGC-1α (as shown in scheme) with GST-tagged human SET7/9 (left) or GST-tagged SWIRM domain of human LSD1 (right).

(legend continued on next page)

RNA methyltransferases NSUN2 (Misu), NSUN3, NSUN4, NSUN5 (Wbscr20, Wbscr20a), NSUN6 (NOPD1), and NSUN7 that catalyze the methylation of cytosine to 5-methylcytosine (m^5C). This modification appears to be ubiquitous (Squires et al., 2012), yet its significance is poorly understood. NSUN5 and NSUN7 have been linked to organism lifespan in yeast (Schosserer et al., 2015) and male sterility, respectively (Harris et al., 2007; Khosronezhad et al., 2014). Moreover, *NSun7* is highly expressed during murine embryogenesis where energy needs are considered high (Chi and Delgado-Olguín, 2013). At the molecular level, m^5C methylation by NSUN2 in tRNAs and within the 3′UTR of the *INK4A* mRNA promotes stability by abrogating RNA cleavage (Khoddami and Cairns, 2013; Tuorto et al., 2012; Zhang et al., 2012) and in non-coding RNA (ncRNAs) controls the processing of vault ncRNAs into small regulatory RNAs (srRNAs) (Hussain et al., 2013). Conversely, combined loss of *NSun2* and *Dnmt2* in mouse genetic models leads to early embryonic lethality through disruption of the protein synthesis pathway because tRNAs are lost (Tuorto et al., 2012).

Here, we demonstrate that PGC-1α is a substrate for both LSD1 and SET7/9. Lysine methylation of PGC-1α is directed at the residue K779 and appears selectively coupled to eRNAs with increased retention of the Spt-Ada-Gcn5-acetyltransferase (SAGA) complex component CCDC101/SGF29, and Mediator 1 and 17. Loss of *Set7/9* diminished the capacity to retain the SAGA/ Mediator complex, and consequentially diminished the capacity of PGC-1α to stimulate transcription. Selective ablation of these eRNAs in mouse hepatoma cells and primary hepatocytes corresponded with diminished expression of their associated genes. Therefore, interactions between PGC-1α and NSUN7 appear to account for the enrichment of m^5C-modified eRNAs at enhancers of specific target genes, which fine-tunes RNA polymerase II activity to metabolic cues. Moreover, enrichment of m^5C within these specific eRNA species coincides with metabolic stress of fasting in liver in vivo. We therefore link intergenic and eRNAs with post-translationally modified PGC-1α and the transcriptional program of an adaptive metabolic response.

RESULTS

Identification of LSD1 Substrates

Several protein lysine methyltransferases and demethylases have been identified to have critical roles in non-histone proteins, affecting human pathogenesis (Hamamoto et al., 2015). To identify specific substrates of LSD1 in Hepa 1-6 cells we used short hairpin RNAs (shRNAs) targeting the expression of murine *Lsd1* (Figure 1A) following stable isotope labeling by amino acids in cell culture (SILAC) assay. PGC-1α was identified among twenty-seven candidate gene products with a spectra profile that had a strong preference for monomethylated and dimethylated lysine 779 (K779me1 > K779me2 > K779me0) (Figure 1A). To determine if K779 methylation was a specific post-translational modification of PGC-1α, we directed lysine and arginine methyltransferase activities toward the recombinant C terminus of human PGC-1α in vitro, containing the K779 residue. Results revealed that K779 of PGC-1α was preferentially methylated by PRMT1 and SET7/9, whereas G9a, SUV39H1, or PRMT4 failed to methylate this substrate (Figure 1B). Furthermore, we sought to determine if LSD1 could reverse the abundance of [^{14}C]-methylated PGC-1α species on a stoichiometric basis. Hence, we titrated up to 3-fold molar equivalent of recombinant LSD1 with SET7/9 and PGC-1α (Figure 1B) and demonstrated the competing activities between SET7/9 and LSD1 on the C terminus of PGC-1α. To determine the efficiency of SET7/9-mediated PGC-1α[K779] methylation, a constant amount of SET7/9 and ^{3}H [AdoMet] was incubated with increasing amounts of either wild-type (PGC-1α[K779]) or mutant synthetic peptides in which K779 was replaced by an arginine (PGC-1α[K779R]). We found that the reaction rate curve for the wild-type PGC-1α[K779] was higher than for the mutant PGC-1α[K779R] peptide (Figure 1C), suggesting that the lysine K779 of PGC-1α is an efficient and specific substrate for SET7/9. The model structure of the PGC-1α[K779] peptide accommodated in the catalytic pocket of SET7/9 enzyme is shown in Figure S1A.

Direct Interactions with PGC-1α Are Shared between SET7/9 and the SWIRM Domain of LSD1

To further study the nature of PGC-1α interaction with LSD1 and SET7/9, we performed binding assays with recombinant proteins corresponding to various C-terminal fragments of PGC-1α fused to the polyhistidine tag of pET28b, and GST-tagged SET7/9 or the SWIRM domain of LSD1. PGC-1α directly bound to SET7/9 and the SWIRM domain of LSD1 in vitro (Figure 1D) and in vivo, as this interaction was also detected in a native cellular context (Figure S1B). To determine the nature of lysine methylation of PGC-1α, we conducted direct in vitro methylation reactions with either wild-type or mutant SET7/9 enzyme, and the synthetic peptide PGC-1α[K779]. Essentially, MS analysis revealed enrichment of a single methylated species after 30 min of incubation with the wild-type SET7/9 but not with the mutated recombinant enzyme (Figure 1E). Confirmation of SET7/9 activity was also tested on total native histones (Figure S1C). To examine whether PGC-1α became methylated in vivo, HEK293 cells were transfected with 3XFLAG tagged PGC-1α and incubated with L-[methyl-3H]methionine as a traceable methyl donor. The experiment was performed in the presence or absence of the homocysteine hydrolase inhibitor adenosine dialdehyde (AdOx) that blocks generation of the

(E) MS of the in vitro methylation assay of PGC-1α[K779] synthetic peptide with the wild-type or the catalytically inactive SET7/9 enzyme.
(F) HEK293 cells were transfected with triple FLAG-tagged human PGC-1α and cultured with L-[methyl-^{3}H]methionine, in the presence or absence of adenosine dialdehyde (AdOx), cycloheximide (CHX), and chloramphenicol (CA). Inhibition of translation was monitored by labeling cells with [^{35}S] methionine. After metabolic labeling, 3XFLAG/hPGC-1α was immunoprecipitated with anti-FLAG M2 beads and depicted with fluorography.
(G) Schematic diagram illustrating the luciferase-coding gene under the control of Gal4 upstream activating sequences (UAS, pG5luc). The pG5luc reporter construct was transfected with the expression vector encoding wild-type PGC-1α, the C-terminal deletion of PGC-1α (ΔC-term) or the mutant PGC-1α (K779R), fused to the Gal4 DNA binding domain (left). Luciferase activity was measured 48 hr after transfection. ChIP for pan-acetyl H3 and GAL4 was performed in parallel from transfected cultures using primers overlapping the GAL4 UAS (right).

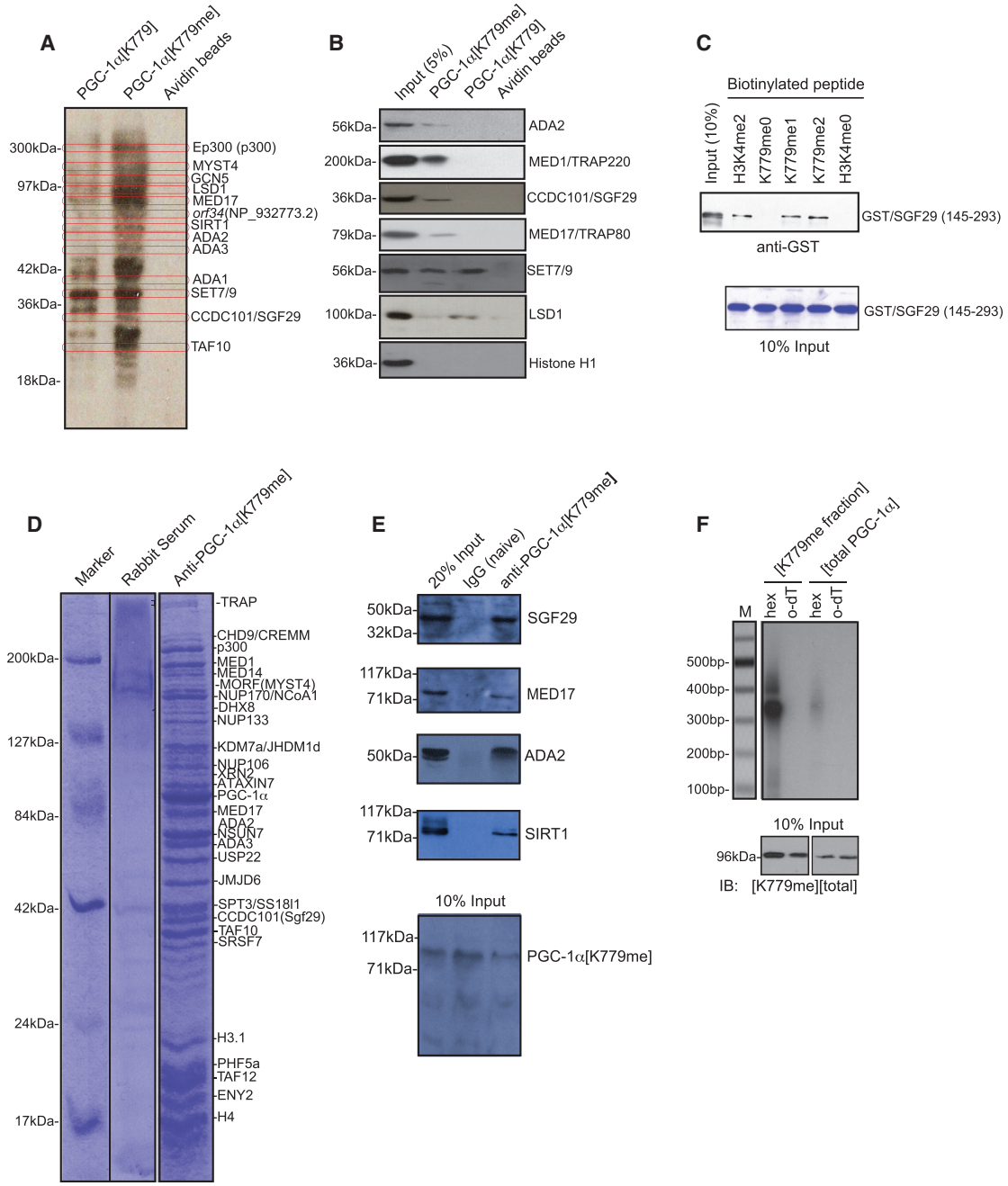

Figure 2. Identification of the Nuclear Methylated PGC-1α[K779me1] Complex

(A) Biotinylated PGC-1α[K779] and PGC-1α[K779me1] synthetic peptides were immobilized on avidin beads and incubated with nuclear extracts of Hepa1-6 cells labeled with [^{35}S] methionine. Parallel PAGE was performed and depicted with fluorography or gel bands excised for peptide identification by MS/MS analysis.

(B) Peptide pull-down of PGC-1α[K779] or methylated PGC-1α[K779me] peptides with nuclear extracts from Hepa1-6 cells. Immunoblot with specific antibodies are shown. Avidin beads were used as control.

(C) Peptide pull-down of PGC-1α[K779], PGC-1α[K779me1], PGC-1α[K779me2], H3K4me0, or H3K4me2 with the GST-tagged tandem tudor domain of the SAGA complex component CCDC101/SGF29 (residues 143–293). Immunoblot with GST antibody (upper) and Coomassie blue staining of the input used (lower).

(D) Coomassie blue staining of proteins eluted by anti-PGC-1α[K779me] immunoaffinity columns. The lanes were sectioned, digested with trypsin, and the extracted peptides were sequenced by mass spectrometry. The positions of molecular mass markers are indicated on the left. Naive rabbit IgG was used as a control shown in the center lane.

(legend continued on next page)

cellular methyl donor S-adenosyl-methionine (Pless et al., 2008) and in the presence of cycloheximide and chloramphenicol to block protein synthesis. Metabolic labeling with ^{35}S-methionine was used as a control for the inhibition of protein translation in the presence of cycloheximide and chloramphenicol (Figure 1F, right). Immunoprecipitation of PGC-1α revealed a ^{3}H-methyl labeled PGC-1α product in the absence but not in the presence of AdOx (Figure 1F, left and middle). To assess the transcriptional activity of PGC-1α, we used a heterologous promoter fused with the Gal4 DNA-binding domain. Loss of the C-terminal domain of PGC-1α as well as mutant PGC-1α[K779R] led to a decrease in the luciferase activity (Figure 1G, left), which was accompanied with a decrease in the abundance of histone H3 acetylation at the upstream activating sequences (UAS) of the GAL4 promoter (Figure 1G, right).

Enrichment and Characterization of the PGC-1α [K779me] Complex

To purify the K779 methyl-specific PGC-1α complex, we used a combination of affinity and immunoaffinity chromatography. Hepa 1-6 cells were incubated with [^{35}S]-methionine and the nuclear extracts were immunoprecipitated with two discrete biotinylated synthetic peptides corresponding to the unmodified C-terminal of human PGC-1α (PGC-1α[K779]) and a peptide bearing a specific monomethylated K779 (PGC-1α[K779me1]). The eluted proteins were electrophoretically separated, depicted with fluorography, and the excised bands were subjected to tandem mass spectrometry (MS/MS) analysis. Methylated PGC-1α[K779me1] peptide specifically bound to components of the SAGA complex (CCDC101/SGF29, ADA2, ADA3) and Mediator (MED1 and MED17) (Figure 2A). The selectivity of these interactions was tested by peptide pull-down experiments (Figure 2B). Prominent among the proteins identified was CCDC101/SGF29, which was previously described as a tandem Tudor domain containing protein selective for H3K4me2/3 binding in human and *S. cerevisiae* (Bian et al., 2011). We then tested the binding of the recombinant Tudor domain of CCDC101/SGF29 with different peptides corresponding to methylated and unmodified species of the C-terminal of PGC-1α and found a selective binding for PGC-1α[K779me1] and PGC-1α[K779me2]. H3K4me2 was used as a positive control (Figure 2C). Peptide pull-down experiments showed that the Mediator component MED17 selectively bound the methylated PGC-1α[K779me1] but not the PGC-1α[K779] peptide in Hepa 1-6 and 3T3L1 cell lines (Figure S2A).

To assess the robustness of these interactions, Hepa 1-6 extracts were subjected to two purification steps on Phosphocellulose P11 and Q Sepharose columns, followed by size fractionation on a preparative Superose 6 column for a initial enrichment of >200-fold for the complex. This enriched preparation was divided and applied to immunoaffinity column composed of a rabbit polyclonal antibody directed against the methylated PGC-1α[K779me] peptide (Figures S2B–S2E). The eluted proteins were identified using MS analysis and listed alongside the high sensitivity Coomassie blue-stained polyacrylamide gel (Figure 2D). Although the hepatoma Hepa 1-6 cell line with oncogenic properties may provide a distinct composition from the normal hepatocyte, results from published studies illustrated a pool of shared components (Chen et al., 2009; Wallberg et al., 2003). However, several other candidates remained uncharacterized as for example, components of the SAGA complex, as well as some orphaned nuclear pore and RNA processing components as the N^{5}cytosine RNA methyltransferase NSUN7 (Figure 2D). Surprisingly, several Mediator components were absent, suggesting that alternative compositions may exist within a native PGC-1α complex. To assert the authenticity of the interactions we paneled several protein interactions by co-immunoprecipitation experiments (Figure 2E). We further tested the possibility of differential RNA binding by methylated and unmethylated PGC-1α by RNA immunoprecipitation (RIP). The PGC-1α[K779me] fraction strongly retained RNAs, which were suspected to be short ncRNAs as they failed to generate any significant signal from oligo dT mediated reverse transcription of polyadenylated RNA species (Figure 2F).

Genomic Distribution of PGC-1α[K779me]

To ascertain the distribution of chromatin-bound PGC-1α and methylated PGC-1α[K779me] we performed chromatin immunoprecipitation coupled with massively parallel DNA sequencing (ChIP-seq). Because of the suspected avidity of our custom antibody (Figures S2B–S2E), the read depth was substantially greater for the PGC-1α[K779me] than for total PGC-1α, rendering 9,472 and 2,395 called peaks, respectively, that were associated with a significant overlapped number of genes (Figure 3A). The distribution of peaks for PGC-1α[K779me] was slightly shifted 5′ upstream of the TSS when compared with total PGC-1α (Figure 3B), suggesting an accumulation of intergenic peaks nearest the adjacent genetic loci. Overall, the density of PGC-1α[K779me] enrichment still greatly appeared over the TSS, whereas significant enrichment for both species of PGC-1α was found at intergenic sites of neighboring genes (Figure 3C). The genomic distribution of peaks shared between the PGC-1α[K779me] and total PGC-1α was in concordance with previous published studies done in human HepG2 cells (Charos et al., 2012). Most of the overlapped binding sites resided on the promoters and the intergenic region, although a minority of peaks was also localized to the intragenic and 3′ UTR regions (Figure 3D). PGC-1α target genes associated with gene ontology (GO) categories such as positive regulation of transcription, chromatin modification, and PI3/AKT/mTOR signaling, among others (Figure 3E). Furthermore, DNA motifs overrepresented in PGC-1α[K779me] fell into four dominant motif consensus classes, including the TFIID, LXR, NRF2, and the PPAR family of transcription factors (Figure 3F, left and middle), which were

(E) Immunoprecipitation with anti-PGC-1α[K779me] or with naive IgG serum was performed from Hep1-6 hepatoma cell nuclear extracts and immunoblotted for the indicated interacting partners. Immunoblot of PGC-1α[K779me] of the 10% of input used in this assay (lower).

(F) UV crosslinked RNA was immunoprecipitated with methylated PGC-1α[K779me] and total PGC-1α antibodies. The enriched RNA was reverse -transcribed using either oligo-dT (o-dT) or random hexamers primers (hex) and labeled with CTP, [α-^{32}P]. Input level of methylated PGC-1α[K779me] and total PGC-1α is shown below.

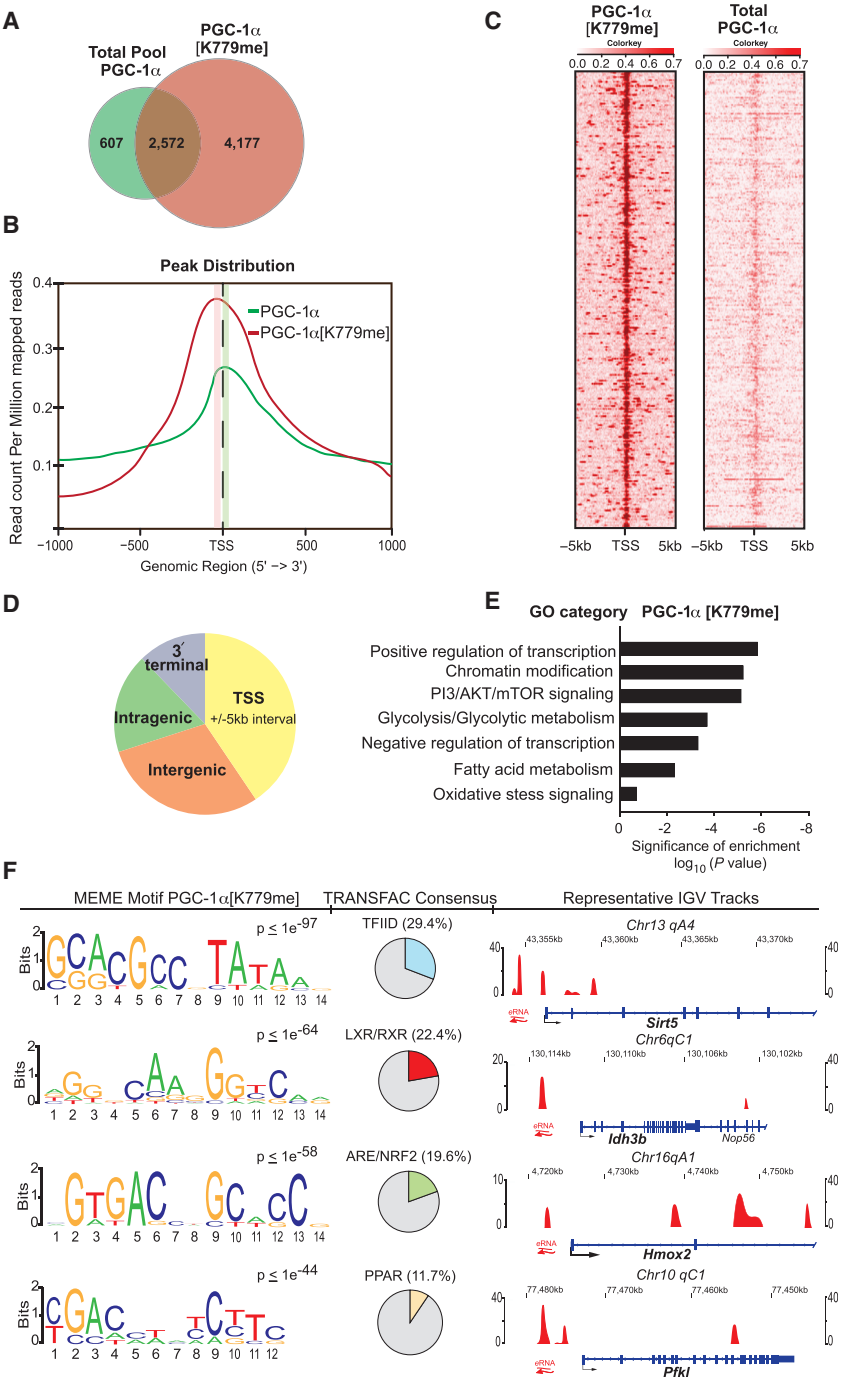

Figure 3. PGC-1α[K779me] Is Associated with Enhancers and Core Promoters of Metabolic Genes

(A) Venn diagram representing the overlap of PGC-1α [K779me] and total PGC-1α bound genes.

(B) Peak distribution of enriched ChIP reads along the annotated transcriptional start sites (TSS) for PGC-1α [K779me] and the total pool of PGC-1α.

(C) Density alignment of ChIP peaks relative to the TSS for PGC-1α[K779me] and unmethylated PGC-1α.

(D) Genome distribution of the overlapped peaks.

(E) Gene ontology analysis of the PGC-1α[K779me] ChIP peaks.

(F) Motif discovery from summit regions from PGC-1α [K779me] ChIP-seq. MEME analysis significantly identified specific transcription factor (TF) motifs (left) with their corresponding p values (top right of motif); TRANSFAC analysis indicates the proportion of TF motifs found among the overall peak distribution (center). Custom IGV tracks of genes represented as sequences enriched for specific TFs derived from the MEME enrichment analysis (right).

localized in four metabolic genes identified as specific targets of *Pgc-1α* by knockdown experiments (Figure 3F, right; Figure S3A): 6-phosphofructokinase (*Pfkl*), Sirtuin 5 (*Sirt5*), isocitrate dehydrogenase 3 (*Idh3b*), and Heme oxygenase (*decycling*) 2 (*Hmox2*). Thus, depletion of *Pgc-1α* led to a decrease of *Pfkl*, *Sirt5*, *Idh3b*, and *Hmox2* expression, which was rescued with wild-type PGC-1α, but not mutated PGC-1α[K779R], overexpression. The known PGC-1α targets *Pepck* and *Mcad* were tested as controls (Figure S3A). The enrichment of PGC-1α [K779me] at these loci was validated by chromatin immunoprecipitation (ChIP)-qPCR in control and *Set7/9* knockdown Hepa 1-6 and differentiated C2C12 cells (Figure S3B).

PGC-1α[K779me] Potentiates Both the Expression of Target Genes and the Corresponding eRNAs Associated to These Loci

To characterize a functional consequence for the methylated species of PGC-1α, we reprogrammed wild-type and *Set7/9* −/− mouse embryonic fibroblasts (MEFs) to induced hepatocytes (iHeps), using a modified described protocol (Sekiya and Suzuki, 2011) (Figure 4A). For a greater efficiency of hepatocyte transformation, the retroviral expression of *Hnf4α*, *Foxa1*, and *Foxa2* was required, as opposed to using a combination of two factors. Note that the reprogramming efficiency of iHeps was not affected upon *Set7/9* loss (Figure S4A). PGC-1α expression was induced in iHeps even in the absence of *Set7/9*, whereas methylated PGC-1α[K779me] was depleted in the absence of *Set7/9* when compared to the total pool of PGC-1α (Figures 4B and 4C). Moreover, markers of definitive hepatocyte differentiation, such as *Ntcp* and *Bsep*, and the nuclear receptor *Rxrα* became more evident (Figures S4B and S4C) confirming the status of hepatocyte differentiation. Because PGC-1α[K779me] binding was detected at the active enhancers of the PGC-1α target genes, characterized by an enrichment of H3K27ac and components of the SAGA and Mediator complexes (Creyghton et al., 2010; Kagey et al., 2010), and

was found to show stronger retention of ncRNAs, we tested whether we could detect eRNAs associated with these loci. Thus, specific primers for each PGC-1α[K779me] enriched peak upstream of the associated TSS were designed and used for measuring the transcript abundance. We detected the expression of eRNAs associated to *Pfkl*, *Sirt5*, *Idh3b*, and *Hmox2* genes, which was drastically abolished upon *Set7/9* loss (Figure 4D, right). The changes in eRNA expression levels strongly correlated with changes in mRNA expression of the nearby genes (Li et al., 2013) (Figure 4D, left), although the effect was more moderate. Furthermore, knockdown of *Set7/9* in Hepa and differenciated C2C12 cells was accompanied with a decrease in the binding of PGC-1α[K779me], MED1, MED17, and CCDC101/SGF29 at the enhancer of these loci (Figure S3B), suggesting that methylated PGC-1α[K779me] was essential for the recruitment of Mediator and SAGA complexes at the enhancers of the target genes. Next, we infected cells with wild-type and mutant forms of PGC-1α and showed that only wild-type PGC-1α corresponded with both modest restitution of eRNAs as well as mRNA transcripts corresponding with *Pfkl* and *Sirt5* (Figure S4D), whereas the expression of *Foxm1b*, a marker of hepatocyte identity, was independent of the methylation status of PGC-1α (Figure S4E).

Pfkl-Associated eRNA Is Preferentially Bound by Methylated PGC-1α

We next examined the RNA binding potential of PGC-1α[K779me] with the *Pfkl*-associated eRNA by RIP-Northernblot (Figure 5A). In both Hepa1-6 and C2C12 cell lines a signal between 0.5-1 kb was abrogated after knockdown of *Set7/9* (Figure 5B). This result was confirmed by qPCR using the previously reported *Dlx-6as* enhancer-associated transcript (*Evf-2*) as a negative control for PGC-1α transcript selectivity (Figure 5C) (Berghoff et al., 2013; Feng et al., 2006). Furthermore, we sought to text the binding of the *Pfkl* eRNA with PGC-1α, PGC-1α[K779me], CCDC101/SGF29, and MED1, and the RNA binding proteins HEXIM and LARP7. Thus, nuclear extracts from NIH 3T3 and Hepa1-6 cells were incubated with the RNA probe, and the detected bands were supershifted when PGC-1α, PGC-1α[K779me], CCDC101/Sgf29 and MED1 specific antibodies were added. No binding of *Pfkl*-associated eRNA with either HEXIM or LARP7 was detected, demonstrating selectivity for the engineered ncRNA transcript by PGC-1α and interacting protein subunits (Figure 5D).

NSUN7 Promotes PGC-1α-Mediated Transcription and Corresponds with Enrichment of Specific Enhancer-Associated Transcripts for *Pfkl*, *Sirt5*, *Idh3b*, and *Hmox2*

To gain deeper mechanistic inside of the association between NSUN7 and PGC-1α[K779me] (Figure 2D), we performed immunoprecipitation assays with specific antibodies against total and methylated PGC-1α. Western blot of NSUN7 showed that both PGC-1α and PGC-1α[K779me] species associated with the NSUN7 (Figure S5A), which was corresponded with a strong nuclear co-localization as demonstrated by immunocytochemistry microscopy (Figure S5B). The staining of NSUN7 was not confined at the nucleolus but at the nuclear periphery, suggesting that the subcellular localization maybe linked to the cell cycle and cellular stress (Frye and Watt, 2006). Furthermore, ChIP experiments showed an overlapped binding between methylated PGC-1α[K779me] and NSUN7 at enhancers of PGC-1α target genes (Figures 6A and S5C). Depletion of *NSun7* corresponded with moderately diminished expression of *Pfkl*, *Sirt5*, *Idh3b* and *Hmox2* mRNA, but more abrupt decrease of the associated eRNAs (Figures 6B, S5D, and S5E), suggesting that m^5C RNA mark affects eRNA stability. Additionally, 5-azacytidine-mediated RNA immunoprecipitation (Aza-IP) experiments showed a decrease of m^5C abundance upon *NSun7* depletion at the *Pfkl*, *Sirt5*, *Idh3b*, and *Hmox2* eRNAs, indicating that NSUN7 is the primary methyltransferase for these RNA species (Figures 6C and S5F). RIP assays with NSUN7 antibody and m^5C RNA detection followed by qPCR further confirmed that both stability and presence of the m^5C mark were contingent on *NSun7* expression, whereas, *Evf-2* transcripts were modestly affected (Figure S5G). Moreover, analysis of m^5C in the *Pfkl* and *Sirt5* eRNAs by Methylamp RNA Bisulfite Conversion Kit in Hepa1-6 cells depleted of *NSun7* and/or *Pgc1α* reinforced the hypothesis that eRNAs selectively undergo cytosine modification (Figure 6D).

In Vivo Function of eRNAs and Significance of m^5C RNA Modification

To assess whether the studied eRNAs affected transcription either in *cis* or in *trans*, we performed loss-of-function assays by knockdown of *Pfkl* and *Sirt5*-associated eRNAs. Depletion of *Pfkl* and *Sirt5*-eRNAs was accompanied by a decrease in *Pfkl* and *Sirt5* mRNA levels and protein abundance, respectively (Figures 7A–7C and S6A–S6C), suggesting that these eRNAs affected transcription of neighboring genes, therefore they were functioning in *cis*. Next, we asked whether the *Sirt5* eRNA had the capacity to direct a reporter gene by engineering a trans-activation model similar to what was described (Ørom et al., 2010). Doxycycline-induced transcription of the *Sirt5* eRNA increased *Sirt5* reporter activity greater than 4-fold over the control, indicating that *Sirt5* eRNA had enhancer activities toward *Sirt5* expression (Figure 7D). To further evaluate the physiological function of *Sirt5* eRNA, we tested the lysine deglutarylase activity of SIRT5 upon knockdown of its associated eRNA (Tan et al., 2014). We found that carbamoyl phosphate synthase 1 (CPS1), a specific substrate of SIRT5, was glutarylated upon depletion of *Sirt5* eRNA, leading to an overall diminishment in CPS1 activity (Figures 7E and 7F). Overall, these results suggest that eRNAs are important sensors of the metabolic state.

To further assess the global role of m^5C RNA, we measured *NSun7* and *Sirt1* expression from liver of fasted DBA/2 mice. Results indicated that *NSun7* was elevated upon 18 hr of fasting and corresponded with a global increase of m^5C RNA (Figure 7G), detected by quantification of the total cytosine pool in RNA not converted by bisulfite treatment. We conclude from these findings that m^5C enrichment could be a response to changes in all RNA species, inclusive of tRNAs and rRNAs (Figure S6D), reflecting the stability of these RNA species during metabolic stress. Overall, our work uncovers an unexpected function of ncRNAs for PGC-1α-mediated transcription, shaped by pathways that integrate post-translational modification of

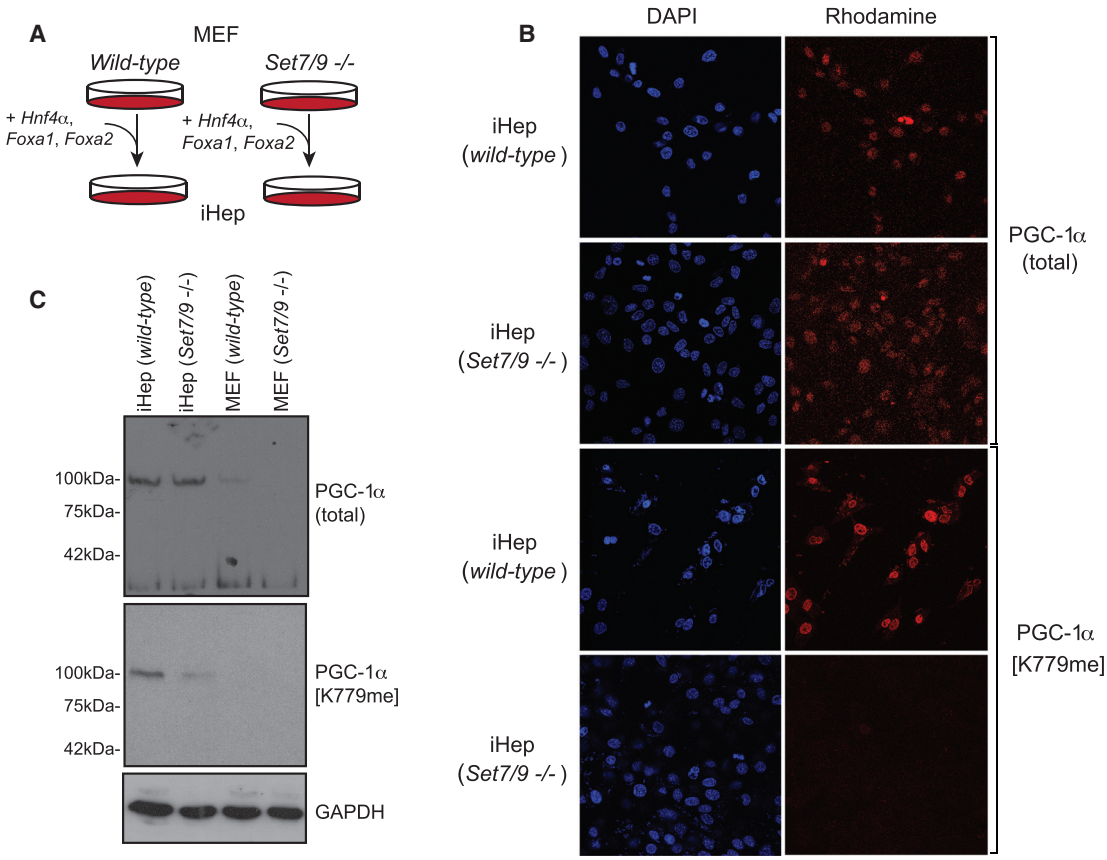

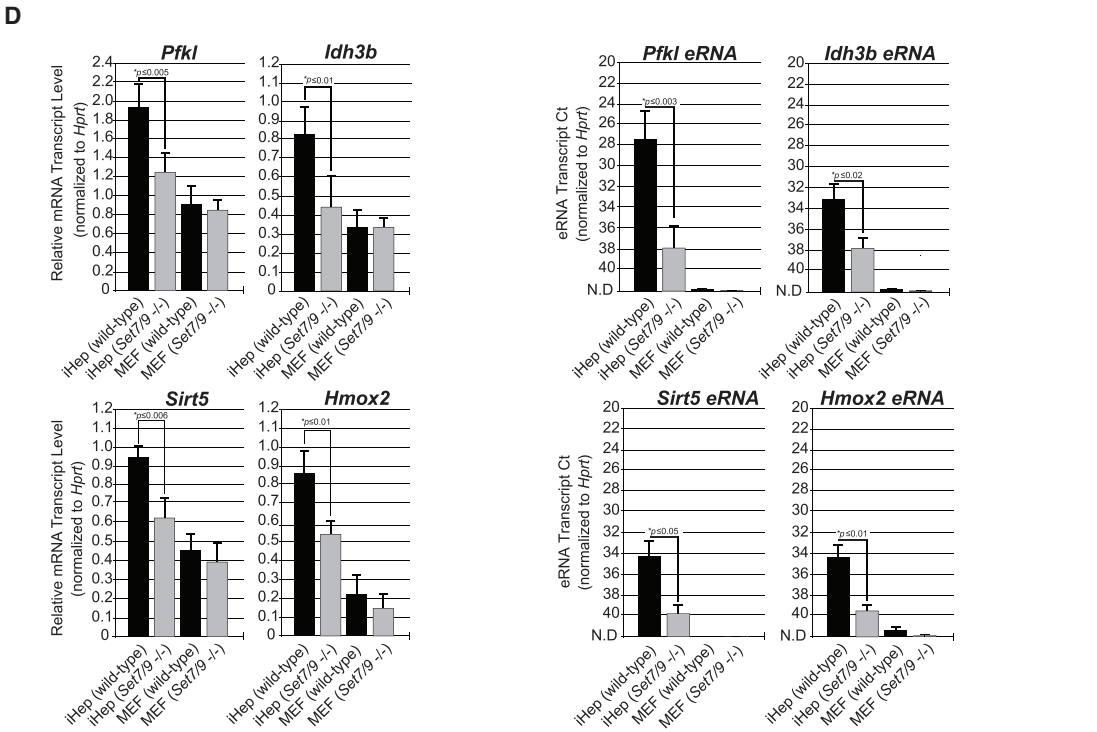

(legend on next page)

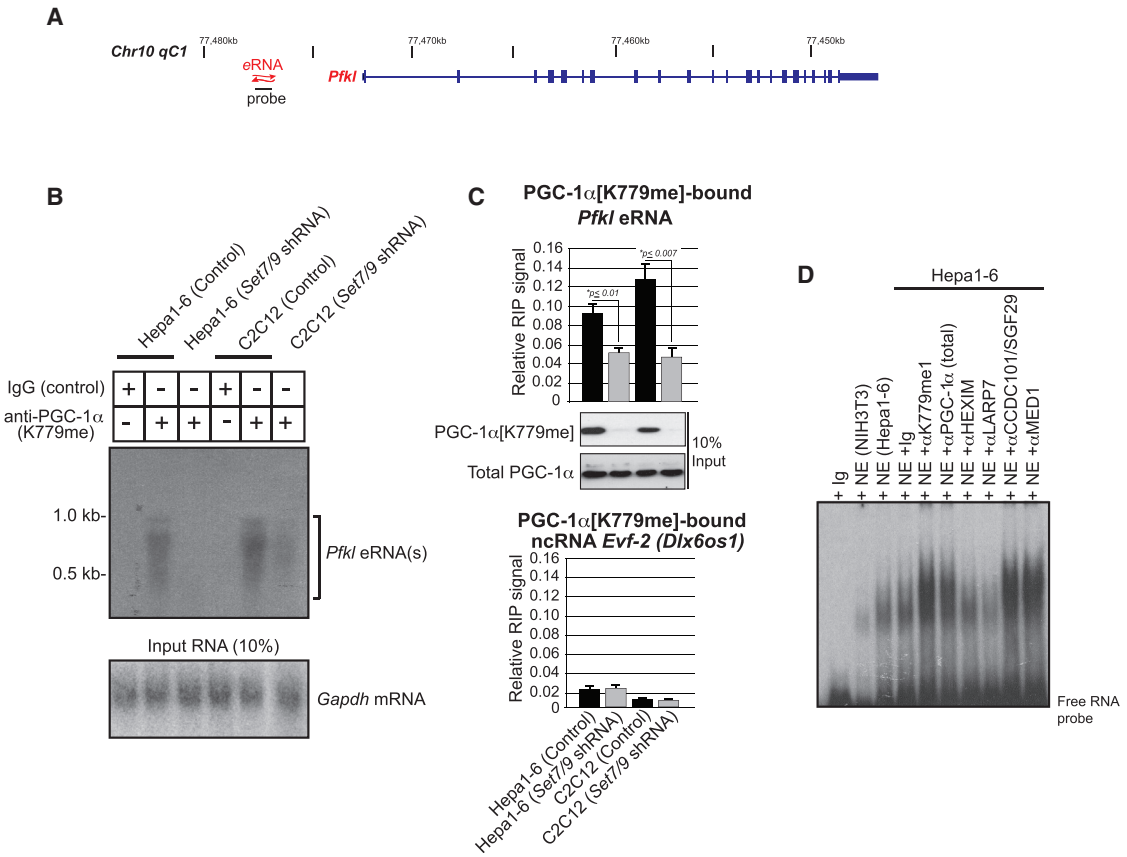

Figure 5. Binding to eRNAs Corresponds with the SET7/9-Mediated Methylated State of PGC-1α

(A) Schematic diagram of the murine *Pfkl* locus. The position of the eRNA probe used in different assays is shown.

(B) Binding of PGC-1α[K779me] to *Pfkl*-associated eRNA was analyzed by RIP Northern blot analysis upon knockdown of *Set7/9* in both Hepa 1-6 and C2C12 cells. Detection of *Gapdh* mRNA was used as a control (lower).

(C) qPCR of the *Pfkl*-associated eRNA and the *Dlx2* enhancer-associated *Evf-2* (*Dlx6os1*) transcript used as a negative control, after RIP with PGC-1α[K779me] antibody upon *Set7/9* depletion in both Hepa 1-6 and C2C12 cells. Shown are the relative abundance for 10% of total input of PGC-1α as a total and methylated K779 fractions.

(D) RNA EMSA using Hepa 1-6 nuclear extracts and the radiolabeled RNA probe corresponding to the *Pfkl*-associated eRNA described in (A). The indicated antibodies were added to detect supershifted bands.

PGC-1α with eRNAs and NSUN7. We suggest these studies will contribute to an emerging understanding of how dynamically modified eRNAs may influence transcriptional responses to adaptive metabolic stress (Figure 7H).

DISCUSSION

The post-translational modifications of PGC-1α and their influence on its transcriptional activity have been well studied (Fernandez-Marcos and Auwerx, 2011), and they are related with the rapid ability to change protein activity and function in response to metabolic stimuli. In this report, we showed that PGC-1α undergoes lysine methylation and demethylation at K779 mediated by SET7/9 and LSD1, respectively. Understanding the mechanism and the consequences of PGC-1α methylation may lead to a mean to modulate PGC-1α activity and intervene in metabolic diseases. The methylated pool of PGC-1α corresponds with the retention of SAGA and Mediator complexes, a number of RNA binding proteins, and with the aggregation of ncRNAs, postulating

Figure 4. Loss of *Set7/9* Contributes to *e*RNAs Depletion

(A) Schematic diagram illustrating the transdifferentiation protocol of wild-type and *Set7/9* null (*Set7/9* −/−) MEFs into induced hepatocytes (iHeps).

(B) Immunocytochemistry analysis of wild-type and *Set7/9* null iHep, using PGC-1α[K779me] and PGC-1α antibodies and rhodamine-labeled anti-rabbit IgG (right). DAPI was used for DNA staining (left).

(C) Western blot of total PGC-1α and PGC-1α[K779me] in wild-type and *Set7/9* −/− iHep and MEFs, respectively. GAPDH was used as a loading control.

(D) qPCR assays of the *Pfkl*, *Sirt5*, *Idh3b*, and *Hmox2* mRNA transcripts (left) and the associated eRNAs upstream the TSS (right) in wild-type and *Set7/9* −/− iHep and MEFs.

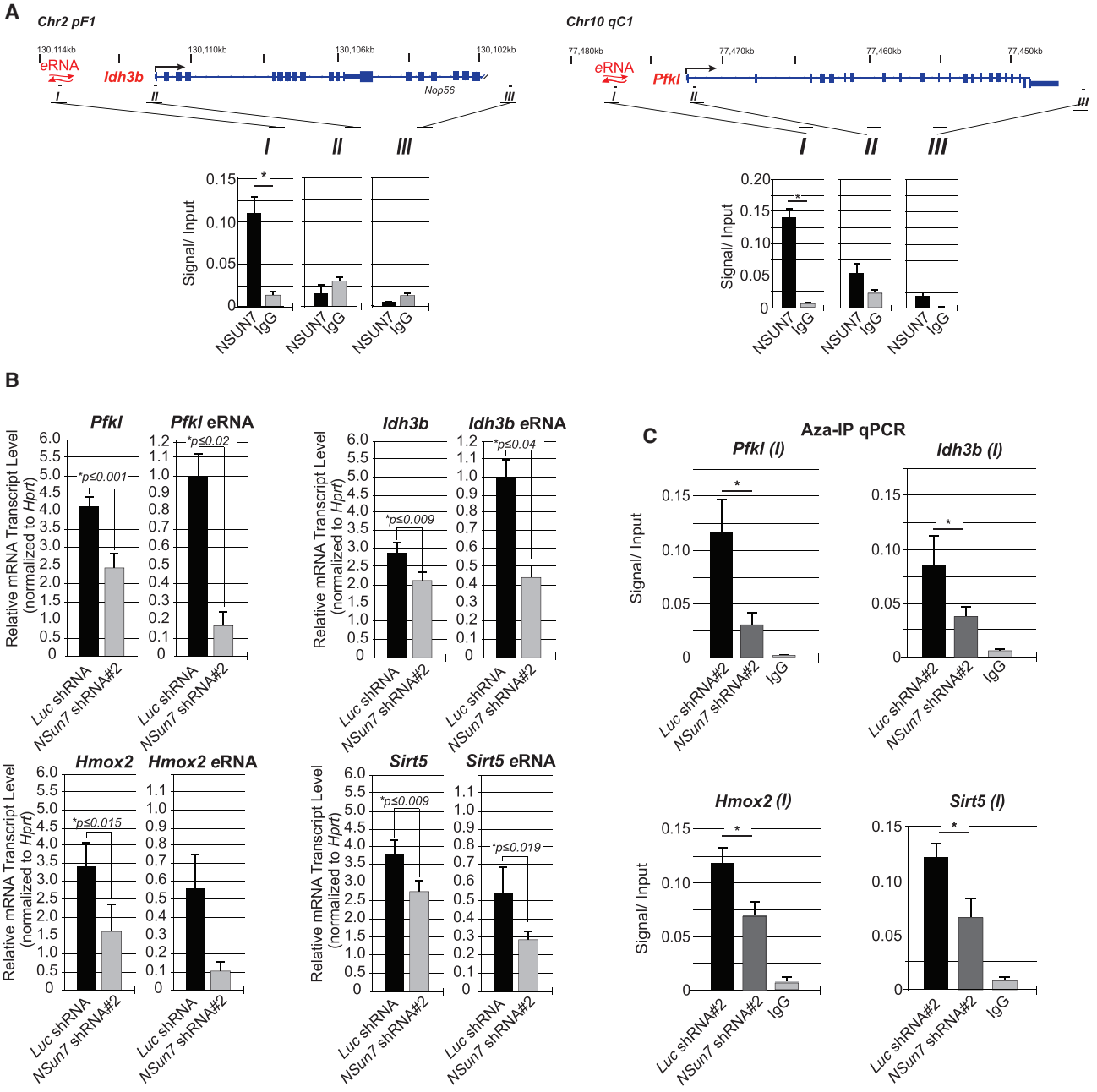

(legend on next page)

whether this feature of PGC-1α activity is linked to its control of transcription.

To reveal specific methylated and unmethylated PGC-1α target genes, we conducted ChIP-seq studies in Hepa1-6 cells. Our analysis revealed some discrepancies in the number of peaks for PGC-1α and PGC-1α[K779me], likely indicating the poor avidity of the commercial antibody used in our ChIP experiments. In contrast, the custom antibody raised against methylated PGC-1α[K779me] was optimized for ChIP studies and seemed to reflect the depth of coverage of the methylated species over the total PGC-1α targets. Nonetheless, we were cautious as our interpretation was shape primarily around the PGC-1α[K779me] ChIP-seq data. Moreover, results from the GO ranking primarily activating genes involved in positive regulation of transcription validated our approach and confirmed the quality of the dataset. Direct knockdown studies combined with ChIP analysis revealed some bona fide targets as *Pfkl*, *Sirt5*, *Idh3b*, and *Hmox2* genes. Although a significant pool of PGC-1α[K779me] resides within the TSS, we were able to localize a significant binding at enhancer regions that allowed the characterization of eRNAs overlapping those PGC-1α[K779me] peaks. Thus, complex ncRNA-protein interactions appear consequential to the fidelity of transcription and to the cellular metabolic fate. While the expanded roles of ncRNAs together with RNA-binding, -processing, and -modifying proteins are emerging as regulators of RNA polymerase II-directed transcription (Nagaike et al., 2011), none of the published studies have illustrated a precise mechanism for eRNA function (Natoli and Andrau, 2012). Here, we provide an unexpected concept for metabolic regulation by PGC-1α corresponding with eRNAs under a methylation specific context. Therefore, in iHep *Set7/9* −/− the expression of these eRNAs was almost abolished. Furthermore, the binding of PGC-1α[K779me], Mediator and the SAGA component CCDC101/SFG29 at the target genes was drastically decreased upon *Set7/9* knockdown. While the total PGC-1α pool certainly contains bound RNA the enrichment with PGC-1α[K779me] suggests a regulatory mode for PGC-1α post-translational modification. The fact that PGC-1α uses RNA in control of transcription is not unexpected due to its well-conserved RRM and the previously assumed nature of PGC-1α tightly coupled with RNA processing (Monsalve et al., 2000). However, the range of RNA bound by PGC-1α, together with the role of methylated PGC-1α, provide new insight regarding the RNA species that may be involved with metabolic homeostasis.

Our notion that m^5C modification of RNA may be coupled with tRNA, polyadenylated mRNA, and ncRNA stability adds further complexity to a regulatory mechanism imposed through eRNA species as an additional class of ncRNAs. Thus, *NSun7* depletion corresponded with a loss of m^5C on the *Pfkl*-, *Sirt5*-, *Idh3b*-, and *Hmox2*-associated eRNAs. Furthermore, specific PGC-1α peaks may suggest that eRNA abundance and turnover are altered as a result of the depletion of m^5C on the measured transcript. However, the molecular basis of this is not yet evident. It is plausible to consider that PGC-1α may also respond to depleted (or elevated) pools of tRNA charged with amino acids and their corresponding m^5C status as a means to sensitize transcriptional mechanisms of available amino acid pools that can accommodate or adapt to metabolic states involved with protein production. This is reminiscent of the simple bacterial model system exploiting tryptophan attenuation of transcriptional elongation (Babitzke, 2004). Although we have no specific evidence of such a mechanism for PGC-1α, previous findings indicate that the majority of substrates for NSUN2, the close homolog of NSUN7, are tRNAs with a distinct population of polyadenylated mRNAs and ncRNAs (Hussain et al., 2013; Khoddami and Cairns, 2013). Moreover, new evidence suggests that the cytosine methyltransferase activity of NSUN5 influences the lifespan in lower eukaryotes by altering rRNA and consequently ribosome stability (Schosserer et al., 2015). Therefore, like their tRNA and rRNA counterparts, the status of eRNAs marked with m^5C could be in the direct response to metabolic stress and provide a greater opportunity to fine-tune responses to these rapid changes through the transcriptional co-activator function of PGC-1α. This notion is consistent with our results showing that overall m^5C RNA abundance and *NSun7* expression are altered in liver during fasting in vivo, and that SIRT5 deglutarylase activity on CPS1 is disrupted upon *Sirt5* eRNA depletion.

EXPERIMENTAL PROCEDURES

Detailed experimental procedures are provided in the Supplemental Experimental Procedures. The IACUC approval was granted through protocol 09-0976.

Cell Culture and Inducible Hepatocyte Reprogramming

Cell lines used in this study were obtained from American Type Culture Collection (ATCC) and cultured according to the supplier's recommendations. To induce the differentiation of C2C12 myoblasts, confluent cells were cultured in low-serum differentiation medium (DMEM, 2% horse serum, and 1 μM insulin), and fresh differentiation medium was changed every 24 hr. For ChIP and RNA studies, ~7×10^7 cells and 2×10^6 cells were used, respectively. Mouse embryonic fibroblasts (MEFs) were derived from 13.5-day-old embryos from wild-type and *Set7/9* −/− mice, corresponding to the C57Bl/6 strain background (Kurash et al., 2008). Programming of MEFs into induced hepatocytes was performed essentially as previously described (Sekiya and Suzuki, 2011).

Enhancer-Associated RNA Depletion with LNA-Gapmers

LNAs targeting murine *Pfkl* and *Sirt5* enhancer-associated RNAs or a scrambled negative control sequence were designed, synthesized, and supplied by Exiqon. Detailed LNA sequences used in the eRNA depletion experiments will be provided upon request.

Figure 6. The NSUN7 RNA Methyltransferase Influences PGC-1α Target Gene Expression

(A) ChIP-qPCR of NSUN7 performed on three discrete regions of the *Pfkl* and *Idh3b* loci as shown in the diagram.

(B) Knockdown of *NSun7* results in downregulation of *Pfkl*, *Sirt5*, *Idh3b*, and *Hmox2* mRNA and the associated eRNAs.

(C) qPCR of eRNAs captured by Aza-IP with NSUN7 or IgG control in wild-type and *NSun7* shRNA Hepa1-6 cells.

(D) Bisulfite conversion identified specific unconverted N^5-methylcytosine in the *Pfkl* and *Sirt5* eRNAs dependent on the presence of NSUN7 and mediated through PGC-1α. Hepa1-6 were depleted of *Pgc1α* and *NSun7* by shRNA and the total RNA was subjected to bisulfite treatment. Two individual biological replicates as total RNA were analyzed (n = 2).

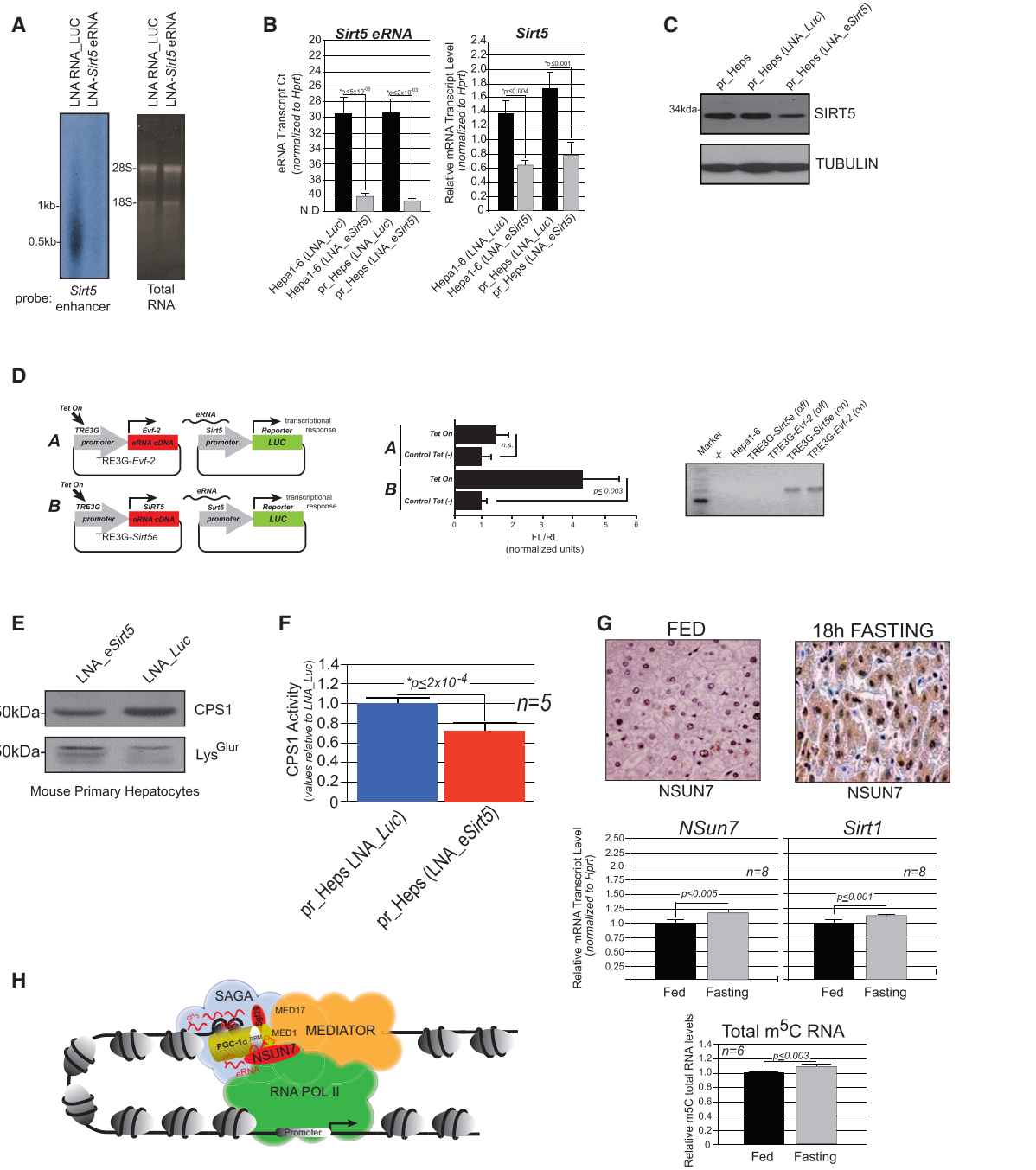

Figure 7. Physiological Function of *Sirt5* eRNA

(A) Northern blot analysis of *Sirt5* eRNAs in control and following eRNA depletion with antisense LNA RNAs (LNA-*Sirt5*) in mouse primary hepatocytes (left). Total RNA was depicted with ethidium bromide under UV transillumination (right).

(B) *Sirt5* eRNA (left) and mRNA (right) qPCR analysis in control and *Sirt5* eRNA-depleted Hepa1-6 hepatoma cells and primary mouse hepatocytes.

(C) Western blot of SIRT5 in control and following depletion of the corresponding eRNAs in primary mouse hepatocytes. TUBULIN was used as a loading control (lower).

(D) Schematics illustrating Tet-On inducible promoter in TRE3G (Clontech) to drive transcription of *Evf-2* and *Sirt5* eRNAs, respectively (left). Graph showing the normalized luciferase activity of the *Sirt5* reporter co-transfected with TRE3G-Evf-2 or TRE3G-Sirt5 eRNA in the presence or absence of doxycycline as indicated. Endpoint PCR is shown for the Tet On abundance of *Sirt5* and *Evf-2* eRNAs, respectively.

(E) Immunoblots for total CPS1 (upper) and glutaryl-lysine CPS1 (lower) in control and *Sirt5* eRNA-depleted primary mouse hepatocytes.

(F) CPS1 enzyme activity was measure and normalized against the LNA control for luciferase.

(legend continued on next page)

Enhancer-Associated RNA Reporter Assays

The enhancer RNA for the murine *Sirt5* gene was directionally cloned into the pTRE3G Tet-On inducible system (Clontech) (Table S1) according to manufacturer's recommendations. The control *Evf-2* cDNA was also introduced into pTRE3G and used as a negative control. The murine *Sirt5* promoter was generated from mouse Hepa1-6 cell genomic DNA using the primers (forward 5′-TCAGGGACAGAGGAGTCACTTCTC; reverse 5′-CTCTCAGCACCGTGGC CCATGG) and cloned into the pBV-LUC backbone acquired from Addgene. Hepa 1-6 cells were co-transfected with the plasmids described above and luciferase reporter gene assays were conducted as described previously. Induction of eRNA transcription was performed by addiction of tetracycline into medium according to the manufacturer's instructions (Clontech).

Quantitation of 5-Methylcytosine (m^5C) in RNA

Bisulfite conversion of RNA was analyzed with the EZ RNA Methylation Kit (Zymo Research) according to the manufacturer's recommendations.

ACCESSION NUMBERS

The accession number for the sequencing datasets reported in this paper is GEO: GSE57852.

SUPPLEMENTAL INFORMATION

Supplemental information includes Supplemental Experimental Procedures, six figures, and one table and can be found with this article online at http://dx.doi.org/10.1016/j.celrep.2015.12.043.

AUTHOR CONTRIBUTIONS

F.A., S.L., N.B., and M.J.W. conceived the idea for this project and wrote the manuscript. A.S. and F.J.S. edited the manuscript. F.A., S.L., N.B., A.S., S.B., M.R., B.A., and C.-H.C. conducted cell culture, trans-differentiation and reprogramming studies. F.A., N.B., A.V., J.A.W., and M.J.W. performed MS studies and/or analyzed proteomic data. F.A., N.B., S.L., and Fe.Z. generated recombinant proteins for binding studies. S.L. and N.B. performed in vitro enzyme studies and binding studies. F.A., S.L., and N.B. performed ChIP and/or ChIP-seq studies and Fa.Z and W.Z. performed bioinformatic analysis. S.L., F.A., and A.S. performed RNA interference studies and immunobloting. C.Q. and M.-M.Z. generated predicted structural models for SETD7/KMT7a specificity for PGC-1α.

ACKNOWLEDGMENTS

We thank Dr. A. Alonso of the Weill-Cornell College of Medicine's Epigenomic Sequencing Core for advice sequencing and library preparation. We thank Dr. B. Bagley of Bioproximity, LLC, for service and support for SILAC analysis and tandem MS studies. We thank Drs. S. Sekiya and A. Suzuki for plasmid constructs, and Dr. Y. Zhao (University of Chicago) for advice for testing SIRT5 enzyme function. F.A. is supported by the Catalan Agency for Administration of University and Research (AGAUR) under a Beatriu de Pinos postdoctoral fellowship. This research was supported by Senior Scholar Award in Aging (AG-SS-2482-10) to M.J.W. from the Ellison Medical Foundation, awards HL067099, HL103967, and CA154903 from the NIH to M.J.W and DK084434 from the NIH to F.J.S.

Received: August 18, 2015
Revised: November 2, 2015
Accepted: December 5, 2015
Published: January 7, 2016

REFERENCES

Aubert, B., Karyotakis, Y., Lees, J.P., Poireau, V., Prencipe, E., Prudent, X., Tisserand, V., Garra Tico, J., Grauges, E., Martinelli, M., et al.; BABAR Collaboration (2009). Search for dimuon decays of a light scalar boson in radiative transitions Upsilon–>gammaA0. Phys. Rev. Lett. *103*, 081803.

Babitzke, P. (2004). Regulation of transcription attenuation and translation initiation by allosteric control of an RNA-binding protein: the Bacillus subtilis TRAP protein. Curr. Opin. Microbiol. *7*, 132–139.

Berger, S.L. (2002). Histone modifications in transcriptional regulation. Curr. Opin. Genet. Dev. *12*, 142–148.

Berger, S.L. (2007). The complex language of chromatin regulation during transcription. Nature *447*, 407–412.

Berghoff, E.G., Clark, M.F., Chen, S., Cajigas, I., Leib, D.E., and Kohtz, J.D. (2013). Evf2 (Dlx6as) lncRNA regulates ultraconserved enhancer methylation and the differential transcriptional control of adjacent genes. Development *140*, 4407–4416.

Bian, C., Xu, C., Ruan, J., Lee, K.K., Burke, T.L., Tempel, W., Barsyte, D., Li, J., Wu, M., Zhou, B.O., et al. (2011). Sgf29 binds histone H3K4me2/3 and is required for SAGA complex recruitment and histone H3 acetylation. EMBO J. *30*, 2829–2842.

Cantó, C., and Auwerx, J. (2009). PGC-1alpha, SIRT1 and AMPK, an energy sensing network that controls energy expenditure. Curr. Opin. Lipidol. *20*, 98–105.

Charos, A.E., Reed, B.D., Raha, D., Szekely, A.M., Weissman, S.M., and Snyder, M. (2012). A highly integrated and complex PPARGC1A transcription factor binding network in HepG2 cells. Genome Res. *22*, 1668–1679.

Chen, W., Yang, Q., and Roeder, R.G. (2009). Dynamic interactions and cooperative functions of PGC-1alpha and MED1 in TRalpha-mediated activation of the brown-fat-specific UCP-1 gene. Mol. Cell *35*, 755–768.

Chi, L., and Delgado-Olguín, P. (2013). Expression of NOL1/NOP2/sun domain (Nsun) RNA methyltransferase family genes in early mouse embryogenesis. Gene Expr. Patterns *13*, 319–327.

Chuikov, S., Kurash, J.K., Wilson, J.R., Xiao, B., Justin, N., Ivanov, G.S., McKinney, K., Tempst, P., Prives, C., Gamblin, S.J., et al. (2004). Regulation of p53 activity through lysine methylation. Nature *432*, 353–360.

Creyghton, M.P., Cheng, A.W., Welstead, G.G., Kooistra, T., Carey, B.W., Steine, E.J., Hanna, J., Lodato, M.A., Frampton, G.M., Sharp, P.A., et al. (2010). Histone H3K27ac separates active from poised enhancers and predicts developmental state. Proc. Natl. Acad. Sci. USA *107*, 21931–21936.

Estève, P.O., Chin, H.G., Benner, J., Feehery, G.R., Samaranayake, M., Horwitz, G.A., Jacobsen, S.E., and Pradhan, S. (2009). Regulation of DNMT1 stability through SET7-mediated lysine methylation in mammalian cells. Proc. Natl. Acad. Sci. USA *106*, 5076–5081.

Feng, J., Bi, C., Clark, B.S., Mady, R., Shah, P., and Kohtz, J.D. (2006). The Evf-2 noncoding RNA is transcribed from the Dlx-5/6 ultraconserved region and functions as a Dlx-2 transcriptional coactivator. Genes Dev. *20*, 1470–1484.

Fernandez-Marcos, P.J., and Auwerx, J. (2011). Regulation of PGC-1α, a nodal regulator of mitochondrial biogenesis. Am. J. Clin. Nutr. *93*, 884S–890S.

Finck, B.N., and Kelly, D.P. (2006). PGC-1 coactivators: inducible regulators of energy metabolism in health and disease. J. Clin. Invest. *116*, 615–622.

Frye, M., and Watt, F.M. (2006). The RNA methyltransferase Misu (NSun2) mediates Myc-induced proliferation and is upregulated in tumors. Curr. Biol. *16*, 971–981.

(G) Immunohistochemical staining of NSUN7 from paraffin embedded liver sections from mice fed and fasted for 18 hr. qPCR analysis of *NSun7* and *Sirt1* mRNA of livers (large lobe) in control or fasted DBA mice (n = 8). Enrichment of m^5C-RNA was quantified by colorimetric analysis of m^5C nuclear RNA following the same 18 hr fast.

(H) In our proposed model, upon PGC-1α methylation by SET7/9, the interaction with SAGA and Mediator is reinforced. NSUN7 methylation of eRNAs associated with PGC-1α target genes reinforces the stability of the eRNA-bound protein complex.

Hamamoto, R., Saloura, V., and Nakamura, Y. (2015). Critical roles of non-histone protein lysine methylation in human tumorigenesis. Nat. Rev. Cancer *15*, 110–124.

Harris, T., Marquez, B., Suarez, S., and Schimenti, J. (2007). Sperm motility defects and infertility in male mice with a mutation in Nsun7, a member of the Sun domain-containing family of putative RNA methyltransferases. Biol. Reprod. *77*, 376–382.

Hussain, S., Sajini, A.A., Blanco, S., Dietmann, S., Lombard, P., Sugimoto, Y., Paramor, M., Gleeson, J.G., Odom, D.T., Ule, J., and Frye, M. (2013). NSun2-mediated cytosine-5 methylation of vault noncoding RNA determines its processing into regulatory small RNAs. Cell Rep. *4*, 255–261.

Jenuwein, T., and Allis, C.D. (2001). Translating the histone code. Science *293*, 1074–1080.

Kagey, M.H., Newman, J.J., Bilodeau, S., Zhan, Y., Orlando, D.A., van Berkum, N.L., Ebmeier, C.C., Goossens, J., Rahl, P.B., Levine, S.S., et al. (2010). Mediator and cohesin connect gene expression and chromatin architecture. Nature *467*, 430–435.

Kelly, T.J., Lerin, C., Haas, W., Gygi, S.P., and Puigserver, P. (2009). GCN5-mediated transcriptional control of the metabolic coactivator PGC-1beta through lysine acetylation. J. Biol. Chem. *284*, 19945–19952.

Khoddami, V., and Cairns, B.R. (2013). Identification of direct targets and modified bases of RNA cytosine methyltransferases. Nat. Biotechnol. *31*, 458–464.

Khosronezhad, N., Colagar, A.H., and Jorsarayi, S.G. (2014). T26248G-transversion mutation in exon7 of the putative methyltransferase Nsun7 gene causes a change in protein folding associated with reduced sperm motility in asthenospermic men. Reprod. Fertil. Dev.

Knutti, D., and Kralli, A. (2001). PGC-1, a versatile coactivator. Trends Endocrinol. Metab. *12*, 360–365.

Kurash, J.K., Lei, H., Shen, Q., Marston, W.L., Granda, B.W., Fan, H., Wall, D., Li, E., and Gaudet, F. (2008). Methylation of p53 by Set7/9 mediates p53 acetylation and activity in vivo. Mol. Cell *29*, 392–400.

Lerin, C., Rodgers, J.T., Kalume, D.E., Kim, S.H., Pandey, A., and Puigserver, P. (2006). GCN5 acetyltransferase complex controls glucose metabolism through transcriptional repression of PGC-1alpha. Cell Metab. *3*, 429–438.

Li, X., Monks, B., Ge, Q., and Birnbaum, M.J. (2007). Akt/PKB regulates hepatic metabolism by directly inhibiting PGC-1alpha transcription coactivator. Nature *447*, 1012–1016.

Li, W., Notani, D., Ma, Q., Tanasa, B., Nunez, E., Chen, A.Y., Merkurjev, D., Zhang, J., Ohgi, K., Song, X., et al. (2013). Functional roles of enhancer RNAs for oestrogen-dependent transcriptional activation. Nature *498*, 516–520.

Lin, J., Handschin, C., and Spiegelman, B.M. (2005). Metabolic control through the PGC-1 family of transcription coactivators. Cell Metab. *1*, 361–370.

Lowell, B.B., and Spiegelman, B.M. (2000). Towards a molecular understanding of adaptive thermogenesis. Nature *404*, 652–660.

Monsalve, M., Wu, Z., Adelmant, G., Puigserver, P., Fan, M., and Spiegelman, B.M. (2000). Direct coupling of transcription and mRNA processing through the thermogenic coactivator PGC-1. Mol. Cell *6*, 307–316.

Nagaike, T., Logan, C., Hotta, I., Rozenblatt-Rosen, O., Meyerson, M., and Manley, J.L. (2011). Transcriptional activators enhance polyadenylation of mRNA precursors. Mol. Cell *41*, 409–418.

Natoli, G., and Andrau, J.C. (2012). Noncoding transcription at enhancers: general principles and functional models. Annu. Rev. Genet. *46*, 1–19.

Nemoto, S., Fergusson, M.M., and Finkel, T. (2005). SIRT1 functionally interacts with the metabolic regulator and transcriptional coactivator PGC-1alpha. J. Biol. Chem. *280*, 16456–16460.

Nicholson, T.B., and Chen, T. (2009). LSD1 demethylates histone and non-histone proteins. Epigenetics *4*, 129–132.

Ørom, U.A., Derrien, T., Beringer, M., Gumireddy, K., Gardini, A., Bussotti, G., Lai, F., Zytnicki, M., Notredame, C., Huang, Q., et al. (2010). Long noncoding RNAs with enhancer-like function in human cells. Cell *143*, 46–58.

Pless, O., Kowenz-Leutz, E., Knoblich, M., Lausen, J., Beyermann, M., Walsh, M.J., and Leutz, A. (2008). G9a-mediated lysine methylation alters the function of CCAAT/enhancer-binding protein-beta. J. Biol. Chem. *283*, 26357–26363.

Pradhan, S., Chin, H.G., Estève, P.-O., and Jacobsen, S.E. (2009). SET7/9 mediated methylation of non-histone proteins in mammalian cells. Epigenetics *4*, 383–387.

Rodgers, J.T., Lerin, C., Haas, W., Gygi, S.P., Spiegelman, B.M., and Puigserver, P. (2005). Nutrient control of glucose homeostasis through a complex of PGC-1alpha and SIRT1. Nature *434*, 113–118.

Rosenfeld, M.G., Lunyak, V.V., and Glass, C.K. (2006). Sensors and signals: a coactivator/corepressor/epigenetic code for integrating signal-dependent programs of transcriptional response. Genes Dev. *20*, 1405–1428.

Scarpulla, R.C. (2008). Transcriptional paradigms in mammalian mitochondrial biogenesis and function. Physiol. Rev. *88*, 611–638.

Schosserer, M., Minois, N., Angerer, T.B., Amring, M., Dellago, H., Harreither, E., Calle-Perez, A., Pircher, A., Gerstl, M.P., Pfeifenberger, S., et al. (2015). Methylation of ribosomal RNA by NSUN5 is a conserved mechanism modulating organismal lifespan. Nat. Commun. *6*, 6158.

Sekiya, S., and Suzuki, A. (2011). Direct conversion of mouse fibroblasts to hepatocyte-like cells by defined factors. Nature *475*, 390–393.

Shiekhattar, R. (2013). Opening the Chromatin by eRNAs. Mol. Cell *51*, 557–558.

Squires, J.E., Patel, H.R., Nousch, M., Sibbritt, T., Humphreys, D.T., Parker, B.J., Suter, C.M., and Preiss, T. (2012). Widespread occurrence of 5-methylcytosine in human coding and non-coding RNA. Nucleic Acids Res. *40*, 5023–5033.

Tan, M., Peng, C., Anderson, K.A., Chhoy, P., Xie, Z., Dai, L., Park, J., Chen, Y., Huang, H., Zhang, Y., et al. (2014). Lysine glutarylation is a protein posttranslational modification regulated by SIRT5. Cell Metab. *19*, 605–617.

Teyssier, C., Ma, H., Emter, R., Kralli, A., and Stallcup, M.R. (2005). Activation of nuclear receptor coactivator PGC-1alpha by arginine methylation. Genes Dev. *19*, 1466–1473.

Towns, W.L., and Begley, T.J. (2012). Transfer RNA methytransferases and their corresponding modifications in budding yeast and humans: activities, predications, and potential roles in human health. DNA Cell Biol. *31*, 434–454.

Tuorto, F., Liebers, R., Musch, T., Schaefer, M., Hofmann, S., Kellner, S., Frye, M., Helm, M., Stoecklin, G., and Lyko, F. (2012). RNA cytosine methylation by Dnmt2 and NSun2 promotes tRNA stability and protein synthesis. Nat. Struct. Mol. Biol. *19*, 900–905.

Wallberg, A.E., Yamamura, S., Malik, S., Spiegelman, B.M., and Roeder, R.G. (2003). Coordination of p300-mediated chromatin remodeling and TRAP/mediator function through coactivator PGC-1alpha. Mol. Cell *12*, 1137–1149.

Wang, J., Hevi, S., Kurash, J.K., Lei, H., Gay, F., Bajko, J., Su, H., Sun, W., Chang, H., Xu, G., et al. (2009). The lysine demethylase LSD1 (KDM1) is required for maintenance of global DNA methylation. Nat. Genet. *41*, 125–129.

Zhang, X., Liu, Z., Yi, J., Tang, H., Xing, J., Yu, M., Tong, T., Shang, Y., Gorospe, M., and Wang, W. (2012). The tRNA methyltransferase NSun2 stabilizes p16INK^4 mRNA by methylating the 3′-untranslated region of p16. Nat. Commun. *3*, 712.